

## Journal Pre-proofs

Evaluation of catacholase mimicking activity and apoptosis in human colorectal carcinoma cell line by activating mitochondrial pathway of copper(II) complex coupled with 2-(quinolin-8-yloxy)(methyl)benzonitrile and 8-hydroxyquinoline

Arif Ali, Snehasis Mishra, Saima Kamaal, Abdullah Alarifi, Mohd Afzal, Krishna Das Saha, Musheer Ahmad

PII: S0045-2068(20)31777-6  
DOI: <https://doi.org/10.1016/j.bioorg.2020.104479>  
Reference: YBIOO 104479

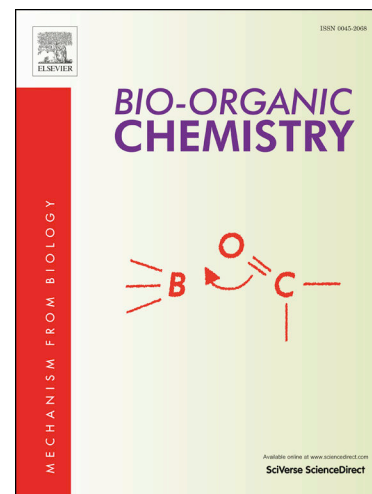
To appear in: *Bioorganic Chemistry*

Received Date: 12 September 2020  
Revised Date: 7 November 2020  
Accepted Date: 12 November 2020

Please cite this article as: A. Ali, S. Mishra, S. Kamaal, A. Alarifi, M. Afzal, K. Das Saha, M. Ahmad, Evaluation of catacholase mimicking activity and apoptosis in human colorectal carcinoma cell line by activating mitochondrial pathway of copper(II) complex coupled with 2-(quinolin-8-yloxy)(methyl)benzonitrile and 8-hydroxyquinoline, *Bioorganic Chemistry* (2020), doi: <https://doi.org/10.1016/j.bioorg.2020.104479>

This is a PDF file of an article that has undergone enhancements after acceptance, such as the addition of a cover page and metadata, and formatting for readability, but it is not yet the definitive version of record. This version will undergo additional copyediting, typesetting and review before it is published in its final form, but we are providing this version to give early visibility of the article. Please note that, during the production process, errors may be discovered which could affect the content, and all legal disclaimers that apply to the journal pertain.

© 2020 Elsevier Inc. All rights reserved.



**Evaluation of catacholase mimicking activity and apoptosis in human colorectal carcinoma cell line by activating mitochondrial pathway of copper(II) complex coupled with 2-(quinolin-8-yloxy)(methyl)benzonitrile and 8-hydroxyquinoline**

Arif Ali,<sup>1</sup>‡Snehasis Mishra,<sup>2</sup>‡ Saima Kamaal,<sup>1</sup> Abdullah Alarifi,<sup>3</sup> Mohd Afzal,<sup>3\*</sup> Krishna Das Saha<sup>2</sup>, Musheer Ahmad<sup>1\*</sup>

<sup>1</sup>*Department of Applied Chemistry, ZHCET, Aligarh Muslim University, Aligarh, 202002, India*

<sup>2</sup>*Cancer & Inflammatory Disorder Division, CSIR-Indian Institute of Chemical Biology, Kolkata 700032, India*

<sup>3</sup>*Department of Chemistry, College of Science, King Saud University, Riyadh 11451, Saudi Arabia*

‡A.Ali and S. Mishra contributed equally to the article.

**Abstract**

To evaluate the cytotoxic potential of metal-based chemotherapeutic candidate towards the colorectal cancer, we have synthesized a new copper(II) complex [Cu(qmbn)(q)(Cl)] (**1**) (where, qmbn = 2-(quinolin-8-yloxy)(methyl)benzotrile and q = 8-hydroxyquinoline) and structurally characterized by single crystal X-ray, Powder-XRD, FTIR and thermogravimetric analysis (TGA). The structural analysis reveals that copper(II) ions exist in a distorted square pyramidal ( $\tau = \sim 0.1$ ), with ligation of a chloride ion, oxygen atom and two nitrogen atoms at equatorial position and one oxygen atom at apical position. The cytotoxicity potential of complex **1** was executed against human colorectal cell lines (HCT116), which showed that **1** induces mitochondrion-mediated apoptotic cell death *via* activation of the Bax (pro-apoptotic protein) caspases-3 and 9 proteins. Interestingly, complex **1** was found to be a good candidate as electron-transfer catalyst which mimics catacholase with high turnover frequency ( $k_{cat} = 1.03 \times 10^2 \text{ h}^{-1}$ ) for the conversion of the model substrate 3,5-di-tertbutylcatechol (3,5-DTBC) to 3,5-di-tertbutylquinone (3,5-DTBQ). Furthermore, molecular docking studies revealed that complex **1** was successfully localized inside the binding pocket of protein kinase (Akt), which validate the mechanism and mode of interaction of **1** that displayed cytotoxic activity experimentally. The obtained outcomes reveal that the complex **1** could be utilized as an encouraging perspective in the development of new therapeutic candidate for colon cancer.

*Keywords:* Copper(II) complex; Single crystal; MTT assay; Molecular docking; Mitochondrial pathway.

## 1. Introduction

Colorectal cancer (CRC), also recognized as large bowel cancer is the third leading cause of cancer death worldwide, and its incidence is gradually rising [1,2]. CRC is a solid tumor arises from the glandular, epithelial cells of the large intestine which encompass aberrant growths in the appendix and large intestine [3–5]. Deplorably, patients with CRC are first detected by oncologists in the metastatic CRC (stage IV); so, that is hard for them to make a widespread recovery [6]. Although innumerable therapeutic regimes such as surgery, chemotherapy has been extensively applied to treat CRC with different curative care. However, the treatment of CRC is restricted by the reduced cytotoxicity of existing chemotherapeutic drugs towards cancer cells due to lack of the tumor suppressor gene p53 [7,8]. The p53 protein is the most crucial tumor suppressor protein defends the cells from acquiring genetic impairment. Nevertheless, the p53 tumor suppressor gene is normally itself mutated during the development of colorectal cancer [9–12]. The activation of p53 gene includes a series of phosphorylation events and post translational modifications which affect the expression of numerous p53-target genes involved in DNA repair, growth arrest, apoptosis, senescence, angiogenesis, and autophagy [13]. Thus, it is necessary to maintain the epithelial integrity and to witness the impression of p53 protein induced by therapeutic candidates is of prime concern. Despite much research and progress made on the expectation of colon cancer, significant inhibition of tumors is still hardly achieved, and the treatment with known agents can lead to tumor progression in some cases also. The early-stage recognition and treatment regimes with proper therapeutic modalities play a pivotal role in reducing the incidence of colon cancer [14,15].

The design and synthesis of metal–organic complexes have attracted remarkable attention for their tunable and functionalized architectures which proves potential therapeutic agent for treating cancer with antioxidant activity [16–23]. Structurally, quinoline-bearing heterocyclic pharmacophores are well-known for their wide range of biological activities such as antifungal [24], antibacterial [25], antitumor [26], and HIV-1 replication inhibitors [27]. Among the quinoline core derivatives, 8-hydroxyquinoline (8-HQ) is the most studied lipophilic metal(II) ion chelator and represents an excellent scaffold with notable features in the area of medicinal applications [28]. Ortiz et al synthesized quinoline-based berberine derivatives, namely NAX012, NAX014, and NAX018 and investigated as promising anticancer drugs for their effects on human colon carcinoma cell lines [29]. Recently, Ai and coworkers reported the newly designed pyrimido[5,4-c]quinoline-4-(3H)-one compounds as possible candidates for cytotoxicity against numerous human cancer cell lines (KB, CNE2, MGC-803, GLC-82, MDA-MB-453, and MCF-7) [30].

In the past few decades, the metal-based drugs have been encouraged after the successful implementation of *cis*-platin and its derivatives for their use in the various kinds of tumors [31]. However, dose-dependent toxicity and resistance coupled with a narrow spectrum of activity associated with these platinum-based drugs restricted their clinical use [32,33]. Therefore, it is pertinent to synthesize a new therapeutic modalities resulting from endogenous transition metal ions, whose mode of action is different from existing platinum based drugs. In this line, copper(II) complexes have been widely studied, which display enhanced cytotoxic profile and reduced toxicity [34–36]. Copper is a physiologically important metal ion that shows a potential role in a redox mechanism and triggers the release of reactive oxygen species (ROS) which induces apoptosis in cancer cells. Copper ions possesses high affinity for nucleobases due to

their selective permeability of cancer cell membranes, hence copper complexes are preferred [37–39]. Additionally, copper has been found to be a part of essential cofactor of several enzymes involved in oxidative metabolism, ceruloplasmine, superoxide dismutase, ascorbic acid oxidase and tyrosinase and so on [40].

In the present article, we have designed and fabricated a new copper(II) complex  $[\text{Cu}(\text{qmbn})(\text{q})(\text{Cl})]$  (**1**). The cytotoxic activity of the complex **1** was investigated against HCT 116 (human colon cancer cell line) to examine its potential as promising chemotherapeutic drugs towards colorectal cancer. Furthermore, catecholase mimics activity of complex **1** has also been explored which shows good turnover frequency number for the conversion of the model substrate 3,5-di-tertbutylcatechol (3,5-DTBC) to 3,5-di-tertbutylquinone (3,5-DTBQ).

## 2. Experimental section

### 2.1. Materials

Reagent grade 2-(bromomethyl) benzonitrile and 8-hydroxyquinoline were purchased from Sigma Aldrich and used as received. All solvents and  $\text{K}_2\text{CO}_3$ ,  $\text{CuCl}_2 \cdot 2\text{H}_2\text{O}$ , KI, NaOH were obtained from Thermo Fisher Scientific, India.

### 2.2. Physical measurements

Infrared spectra were collected (KBr disk,  $4000\text{--}400\text{ cm}^{-1}$ ) utilizing Thermo Scientific iS50 FTIR. Microanalysis was done using a CE-440 elemental analyzer (Exeter Analytical Inc.). Thermal Gravimetric analysis (TGA) was obtained on a Mettler Toledo Star System (heating rate of  $10^\circ\text{C}/\text{min}$ ). Powder X-ray diffraction patterns ( $\text{CuK}_\alpha$  radiation with scan rate  $4^\circ\text{min}^{-1}$  at 298K) were measured from labX XRD-6100 X-ray diffractometer instrument in the range of  $5^\circ\text{--}40^\circ$  at 40kV and 30mA. Uv-visible and photoluminescence spectra were carried out with Thermo

Scientific Evolution 201 UV-visible spectrophotometer and Perkin-Elmer LS55 fluorescence spectrophotometer.

### 2.3. Crystallography

Single crystal X-ray data of complex **1** was collected with a Bruker SMART APEX CCD diffractometer using monochromatic Mo-K $\alpha$  radiation ( $\lambda = 0.71073 \text{ \AA}$ ) at 100(2) K. The linear absorption coefficients, and the anomalous dispersion corrections were mentioned from the International Tables for X-ray crystallography [41]. Using Olex2 [42], the structure was solved with the olex2.solve [43] structure solution program using Charge Flipping and refined with the olex2.refine [43] refinement package using Gauss-Newton minimization. All hydrogen atoms were located in difference Fourier maps in the structures and refined isotropically. All non-H atoms were refined anisotropically. The crystallographic data for complex **1** was summarized in Table 1. Selected bond parameters of complex **1** were given in Table S1.

**Table 1.** Crystal and structure refinement data for complex **1**

CCDC	2003694
Empirical formula	C <sub>26</sub> H <sub>18</sub> ClCuN <sub>3</sub> O <sub>2</sub>
Formula weight	503.45
Temperature/K	100(2)
Crystal system	orthorhombic
Space group	Pbc2 <sub>1</sub>
a/Å	7.9452(7)
b/Å	23.018(2)
c/Å	23.2430(16)
$\alpha$ /°	90
$\beta$ /°	90
$\gamma$ /°	90
Volume/Å <sup>3</sup>	4250.7(6)
Z	8
$\rho_{\text{calc}}/\text{cm}^3$	1.5733
$\mu/\text{mm}^{-1}$	1.184
F(000)	2060.6
Crystal size/mm <sup>3</sup>	0.38 × 0.26 × 0.17

Radiation	Mo K $\alpha$ ( $\lambda = 0.71073$ )
2 $\Theta$ range for data collection/ $^{\circ}$	5.12 to 50
Index ranges	$-10 \leq h \leq 10$ , $-30 \leq k \leq 30$ , $-31 \leq l \leq 31$
Reflections collected	63245
Independent reflections	7484 [ $R_{\text{int}} = 0.2253$ , $R_{\text{sigma}} = 0.1667$ ]
Data/restraints/parameters	7484/1/595
Goodness-of-fit on $F^2$	1.028
Final R indexes [ $I \geq 2\sigma(I)$ ]	$R_1 = 0.0618$ , $wR_2 = 0.1360$
Final R indexes [all data]	$R_1 = 0.1217$ , $wR_2 = 0.1766$
Largest diff. peak/hole / $e \text{ \AA}^{-3}$	0.83/-0.94

### 2.3. Synthesis

#### 2.3.1. Synthesis of 2-(quinolin-8-yloxy)(methyl)benzotrile(qmbn)

8-hydroxyquinoline (2g, 13.7 mmol) and dry  $K_2CO_3$  (5g, 36.17mmol) were mixed in a round-bottom flask containing acetonitrile (60 mL) under an inert atmosphere. The mixture was allowed to stir for 1 hr at  $90^{\circ}C$ . Now, the mixture was added with 2-(bromomethyl)benzotrile (2.69g, 13.7 mmol), and the resulting solution was refluxed for 24h. After completion of the reaction, the solution was allowed to cool at room temperature and poured slowly in ice water (100 mL) with constant stirring to give a white muddy solid precipitate that was collected by filtration and dried under vacuum. Yield: 3.3g (70%). M.P.:  $120^{\circ}C$ . Elemental analysis (%): Calcd. For  $C_{17}H_{12}N_2O$  (260.27): C, 78.44; H, 4.65; N, 10.76%; Found: C, 78.54; H, 4.56, N, 10.71%. IR ( $cm^{-1}$ ): 3398(s), 2924(m), 2922(m), 2824(w), 2224(w), 1619(w), 1564(w), 1503(m), 1463(m), 1379(m), 1324(m), 1262(m), 1177(w), 1100(m), 1027(s), 856(w), 794(m), 753(m), 713(w), 668(w), 547(w). ESI-MS: m/z (100%) 261.1046 [M+1].

#### 2.3.2. Synthesis of complex $[Cu(qmbn)(q)(Cl)] (I)$

A mixture containing ligand (qmbn)(0.02g) and 8-hydroxyquinoline (q) (0.02g) was dissolved in 3 mL methanol in a round bottom flask and added dropwise aqueous solution of  $CuCl_2 \cdot 2H_2O$

(0.08g) and then added 5 drops of NaOH (1 M) solution and allowed to stir for 6h at 90 °C. The resulting solution was cooled down and then filtered. The clear green colored filtrate was kept for evaporation at room temperature. After 2-3 weeks, the green block shape crystals were obtained, which was suitable for single crystal X-ray analysis. Yield: 75%, M.P.: 186 °C. Elemental analysis (%): Calcd. For  $C_{26}H_{18}ClCuN_3O_2$  (503.45): C, 62.03; H, 3.57; N, 8.35%; Found: C, 62.41; H, 3.36, N, 8.25%. IR ( $cm^{-1}$ ): 3380(w), 3215(w), 3033(m), 2921(w), 2817(w), 2229(w), 1658(s), 1614(w), 1572(w), 1502(s), 1462(s), , 1104(s), 818(s), 741(w), 573(m) (Fig. S1).

#### 2.4. Cell lines and chemicals

Cell lines (human colorectal carcinoma, HCT116) were purchased from NCCS, Pune, India. Dulbecco's modified Eagle's medium (DMEM), penicillin–streptomycin–neomycin (PSN) antibiotic, fetal bovine serum (FBS), trypsin and ethylenediaminetetraacetic acid (EDTA) were purchased from Gibco BRL (Grand Island, NY, USA). Tissue culture plastic ware was purchased from NUNC (Roskilde, Denmark). 3-(4,5-Dimethylthiazol-2-yl)-2,5-diphenyltetrazolium bromide (MTT) was procured from SRL, India. Chromium nitrate was bought from Sigma-Aldrich.

#### 2.5. Cell culture

The human colorectal carcinoma cell line HCT116 was cultured in DMEM with 10% fetal bovine serum (FBS) and 1% antibiotic (PSN) at 37 °C in a humidified atmosphere under 5%  $CO_2$ . After 75–80% confluency, the cells were harvested with 0.025% trypsin and 0.52 mM EDTA in phosphate buffered saline (PBS), and seeded at a required density to allow them to re-equilibrate a day before the start of experiment [44].

### 2.6. *MTT assay*

The MTT assay was carried out to estimate the cell viability [45]. The HCT 116 and HEK 293 (Human embryonic kidney 293) were plated in 96-well plates and treated with or without different concentrations of complex **1** for 12h. After 12hr, MTT solution was added and incubated for four hours. After the incubation period of MTT, formazan was solubilized with acidic isopropanol and the absorbance of the solution was measured at 595 nm using an ELISA reader.

### 2.7. *Quantification of apoptosis and necrosis using flow cytometry*

Determination Apoptosis and necrosis were analyzed by flow cytometry using an Annexin-V FITC/PI apoptosis/necrosis detection kit (Calbiochem, CA, USA) [46]. Treated cells ( $1 \times 10^6$ ) were washed and stained with Annexin-V-FITC and PI in accordance with the manufacturer's instructions. The percentages of viable, apoptotic (early and late) along with necrotic cells were estimated by flow cytometry (BD LSR Fortessa, San Jose, CA, USA).

### 2.8. *Determination of intracellular ROS (iROS)*

Mitochondria are the primary source of the amplification of reactive oxygen species (ROS) production in mammalian cells and it plays a major part in the stimulation of apoptosis in a variety of cells [47]. To evaluate the intercellular ROS, we incubated the treated cells with 10  $\mu$ M H2DCFH-DA (2', 7'-dichlorofluorescein diacetate) at 37 °C for 25 min before the analysis by flow cytometer (BD LSR Fortessa, Becton Dickinson, Franklin Lakes, NJ, USA). The increment of DCF fluorescence directly reflects the generated ROS inside cells which were represented as mean fluorescence intensity of DCF [48].

### 2.9. *Assessment of protein localization using immunofluorescence*

HCT 116 cells were plated on cover slips and incubated for 24h. After the incubation period, cells were treated with 9 $\mu$ M complex **1** and incubated for 12h. Untreated was taken as control. After treatment of complex **1**, control/treated HCT 116 cells were washed twice for 10 min each in PBS (0.01 M) and incubated for 1hr in blocking solution containing 2% normal bovine serum, and 0.3% Triton X-100 in PBS. After blocking, the cells were incubated overnight at 4 °C with the respective primary antibody (Bax and cytochrome c) followed by washing and incubation with respective fluorophore-conjugated secondary antibodies for 2 h. The slides were then counterstained with 6-diamidino-2-phenylindole (DAPI) and MitoTracker Red and mounted with the Prolong Anti-fade Reagent (Molecular Probe, Eugene, OR, USA). Stained cells were examined using a confocal laser-scanning microscope (FV 10i, Olympus, Japan) [49].

### 2.10. *Caspase-3/9 activity assays*

Treated cells were exposed to caspase-3 and caspase-9 colorimetric assay using commercially available kits allowing to the manufacturer instruction (BioVision Research Products, Mountain View, CA) respectively [22].

### 2.11. *Scratch assay*

HCT 116 cells were seeded in 6-well plates at the concentration of 2 $\times$ 10<sup>6</sup> cells per well and incubated at 37 °C overnight. Cell monolayers that converged almost 100% were wounded with a sterile 100  $\mu$ L pipette tip. Remove detached cells from the plates carefully with PBS and add DMEM. HCT 116 cells were left either untreated or treated with the indicated doses of complex **1**. After the incubation for 12h, medium was replaced with PBS and the scratched areas were photographed using an Olympus microscope [22].

### 2.12. Statistical analysis

Results were represented as Mean  $\pm$  SEM of the multiple data points. Statistical importance in the deference was calculated by the analysis of variance (ANOVA) using OriginPro (version 8.0) software where  $p < 0.05$  was considered as significant.

### 2.13. Catalytic oxidation of 3, 5-DTBC

The catecholase mimics activity of the complex **1** ( $10^{-4}$  M) was tested with 100 fold of equivalent ratio of 3, 5-di-tertbutylcatechol (3, 5-DTBC) in ethanol as a solvent at room temperature under aerobic condition. The catalytic activity of 3,5-DTBC to 3,5-DTBQ were recorded spectrophotometrically at a wavelength 393 nm using absorbance versus  $\lambda_{\max}$  (nm) plot at 5min time interval. The rate of oxidation of substrate was determined in a concentration dependence manner using 30, 50, 70 and 100 equivalent of substrate as previously reported method [50,51].

### 2.14. Molecular docking

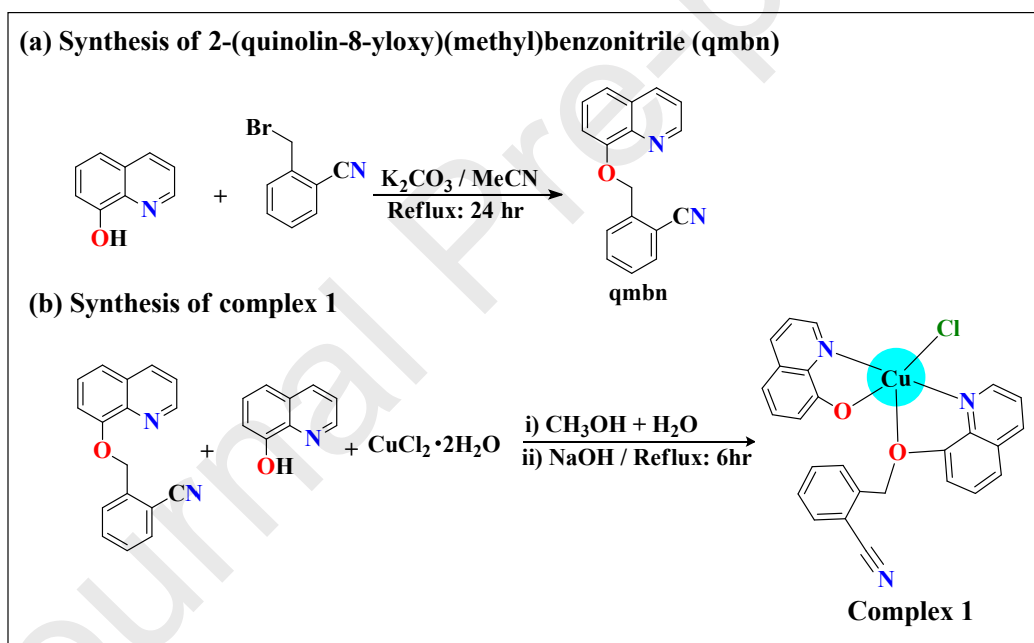
Molecular structure of the complex **1** was generated and optimized using chemical computing In., MOE 2017.09. This structure was then imported to MOE database. 3D crystal structure of Akt-1-inhibitor complexes (PDB ID: 3MVH) having resolution of 2.01 Å was downloaded from protein data bank [52]. Ligand was extracted from 3MVH and prepared for molecular docking. Before optimization, all water molecules were detached through sequence editor of MOE. Complex **1** was optimized and protonated by using MM force field and semi-empirical PM3 methods for docking analysis. After preparation of complex **1** as a drug candidate for the targeted receptor, it was subjected to molecular docking systematic conformational search set at default parameters with RMS gradient of 0.01 kcal mol<sup>-1</sup> employing Site Finder. Several conformational cycles were run in order to get a docked pose as accurate as possible. The best binding pose was chosen based on energetics ground [53]. The interaction energy of drug with 3MVH was

calculated at each step of the docking simulation, whereas, all remaining parameters were fixed at default settings.

### 3. Results and discussion

#### 3.1. Synthesis and general characterization

A new copper(II) complex namely,  $[\text{Cu}(\text{qmbn})(\text{q})(\text{Cl})]$  (**1**) was fabricated with pharmacophore scaffolds 2-(quinolin-8-yloxy)(methyl)benzonitrile and 8-hydroxyquinoline (Scheme 1). The complex **1** was stable towards air and moisture and soluble in water on sonication. The composition of complex **1** was established by microanalytical, TGA, PXRD and FTIR techniques (Fig. S1-S3).



**Scheme 1.** Synthetic scheme for (a) 2-(quinolin-8-yloxy)(methyl)benzonitrile (qmbn) and (b) complex 1.

The bands observed in the FTIR at 2900 and 2229  $\text{cm}^{-1}$  can be attributed to  $\nu(\text{C-H})$  and free nitrile  $\nu(-\text{C}\equiv\text{N})$  stretching absorption frequencies, respectively [54]. The band at 1580  $\text{cm}^{-1}$  could be due to the vibration of pyridine ring of uncoordinated 8-hydroxyquinoline which was

shifted to  $1502\text{ cm}^{-1}$  in the complex **1**. The stretching frequency of  $\nu(\text{Cu-O})$  and  $\nu(\text{Cu-N})$  in the complex **1** was observed at  $655$  and  $570\text{ cm}^{-1}$ , respectively [55] (Table 2 and Fig. S1).

Thermal analysis of CP**1** was carried out in  $\text{N}_2$  atmosphere at the rate of  $10\text{ }^\circ\text{C}$  per minute. Complex **1** exhibited thermal stability upto  $\sim 170\text{ }^\circ\text{C}$ , beyond this temperature framework decomposed (Fig. S2). Moreover, Powder-XRD patterns of complex **1** (experimental or as-synthesized) were in good agreement with the simulated patterns (single crystal-XRD), which confirmed the bulk phase purity of the sample (Fig. S3). Due to different orientations of the crystalline sample, some diffraction peaks were observed with low intensity.

Table. 2. Comparison of selected IR stretching vibration wavenumbers,  $\nu(\text{cm}^{-1})$  between free ligand and complex **1**.

Assignment	Ligand	Complex 1
$\nu\text{C-H}$	2918	2921
$\nu\text{-C}\equiv\text{N}$	2219	2229
$\nu(\text{C=N})$	1619	1614
$\nu(\text{C=C})$	1460	1468
$\nu(\text{Cu-O})$	-	655
$\nu(\text{Cu-N})$	-	570

### 3.2. Structural description

The structure of complex **1** (Fig. 1) has been confirmed by single crystal X-ray diffraction measurement. The complex **1** crystallizes in an orthorhombic crystal system with  $Pbc2_1$  space group. The asymmetric unit contains two crystallographically independent complex units. Each complex unit comprises of one  $q^{-1}$  ligand, one qmbn ligand and one coordinated chloride ion (Fig. 1a). Using Addison's parameter [56], the coordination geometry around Cu1 ( $\tau_5 = 0.106$ ) and Cu2 ( $\tau_5 = 0.145$ ) can be described as distorted square pyramidal. The two equatorial position of each Cu(II) ion is occupied by the O and N atom of  $q^{-1}$  ligand, chloride ion and N atom of the

qmbn ligand. The apical position of the each Cu(II) is coordinated by the O atom of the qmbn ligand (Fig. 1b-c).

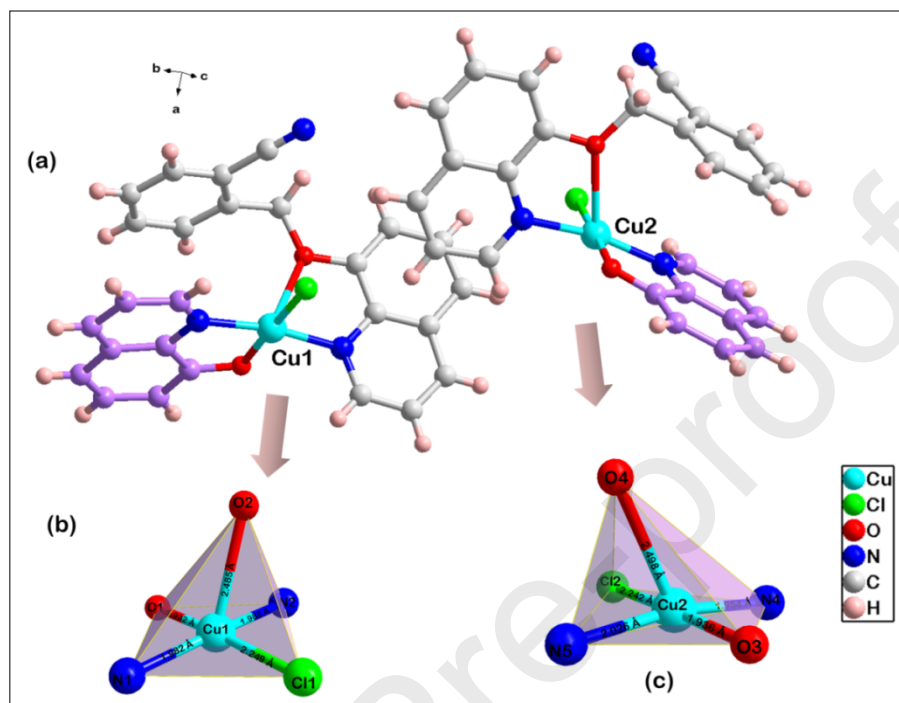


**Fig. 1** Representation of (a) asymmetric unit and (b and c) coordination environment of Cu(II) ions in complex **1**. The C-atoms of ligand Hq is shown in purple color.

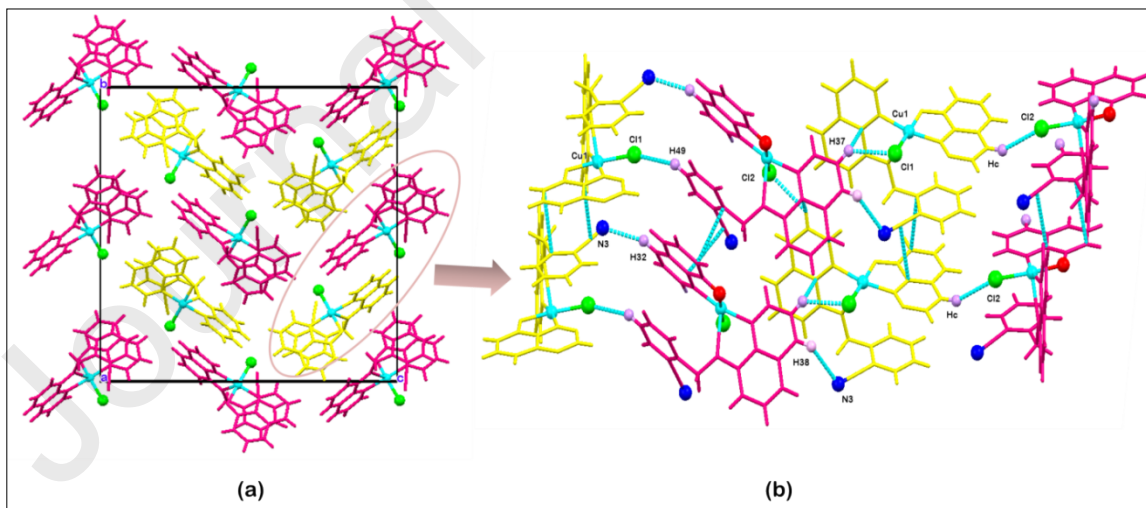


**Fig. 2.** A view of (a) crystal packing showing herringbone pattern along with crystallographic a-axis and (b) supramolecular layers formed *via* H-bonding,  $\pi \cdots \pi$  and C-H $\cdots\pi$  interactions in complex **1**.

The single crystal packing analysis revealed the interesting intermolecular interactions within the crystal system. Each crystallographically independent units of complex **1** are linked through C-H $\cdots$ Cl, C-H $\cdots$ O and C-H $\cdots$ N interactions, and forming 2D herringbone pattern. Further, the intricate array of several  $\pi\cdots\pi$  and C-H $\cdots\pi$  interactions result in the generation of overall 3D supramolecular framework (Fig. 2) [57–59]. The important H-bonding parameters are given in Table 3. However, non-covalent interactions are not only playing a pivotal role in the supramolecular architecture stability but also efficiently interacting with biological systems for diverse functions.

**Table 3** Selected H-bonding parameters in complex **1**.

D-H...A	d(D-H)Å	d(H...A)Å	d(D...A)Å	$\angle$ (D-H...A) $^\circ$
C2-H2...O3	0.93	2.51	3.4261(3)	170
C6-H6...Cl2	0.93	2.74	3.5451(3)	145
C8-H8...Cl1	0.93	2.68	3.2413(3)	119
C28-H28...O3	0.93	2.46	3.3714(3)	166
C32-H32...N3	0.93	2.53	3.3993(3)	157
C34-H34...Cl2	0.93	2.69	3.2378(3)	119
C37-H37...Cl1	0.93	2.76	3.4662(3)	134
C49-H49...Cl1	0.93	2.73	3.5866(3)	154

### 3.3. MTT assay

The well-established MTT assay was used to study the cytotoxicity of the complex **1** at the varying concentrations. At first we have checked the cytotoxicity of the complex **1**, which was evaluated on the human colon cancer cell line (HCT116) and Human embryonic kidney 293 cells (HEK 293) by MTT assay. In case of both the cell line, the dose was selected 0-30  $\mu$ M, for 12hr (Fig.3). The colorimetric data says that, in case of HCT116 cell line at 20  $\mu$ M concentration almost all the cells were death after 12hr of treatment. The data implicated that 30%, 50% and

70% cells were death at 3.68  $\mu\text{M}$ , 9.82  $\mu\text{M}$  and 15.96  $\mu\text{M}$  respectively after 12h of treatment. So we have chosen the  $\text{IC}_{50}$  value (9.82  $\mu\text{M}$ ) for further biological experiments.

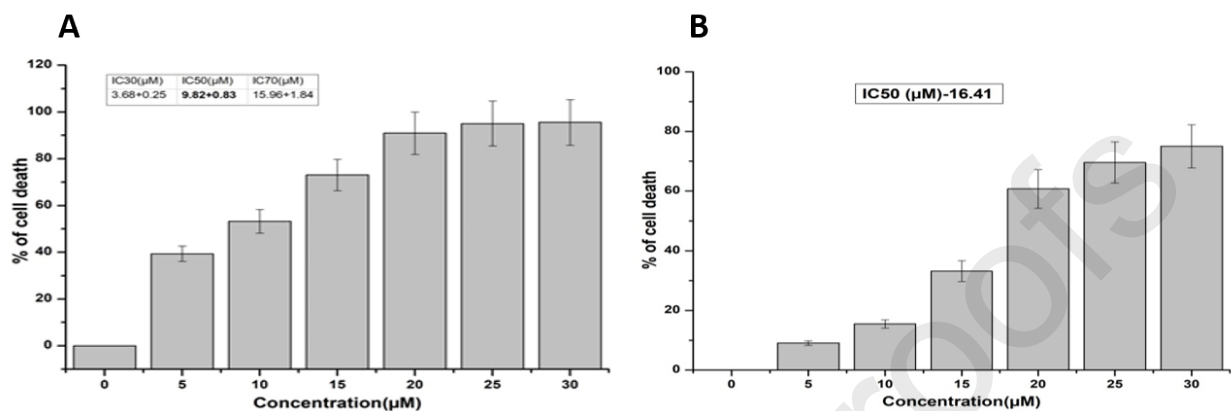


**Fig. 3.** MTT assay data of complex 1 after 12hr of treatment against A. HCT 116 and B. HEK 293 cell line.

#### 3.4. Quantification of apoptosis and necrosis using flow cytometry

To explore whether the complex 1 was involved in apoptosis/necrosis, we conducted flow cytometric assessment using Annexin-V-FITC/PI staining by studying the exposed level of serine phosphatidyl in the outer membrane of cells [60]. The flow cytometric data of Annexin V-FITC-PI assay confirmed that the cell death is occurring due to Apoptosis. The experimental results showed that the cell death is increasing in time dependent manner after treatment of 9  $\mu\text{M}$  complex 1 (Fig. 4). The treatment was given for 12 and 24h duration. These results suggested that complex 1 induced cell death was directly correlated with cytotoxicity followed by apoptosis.

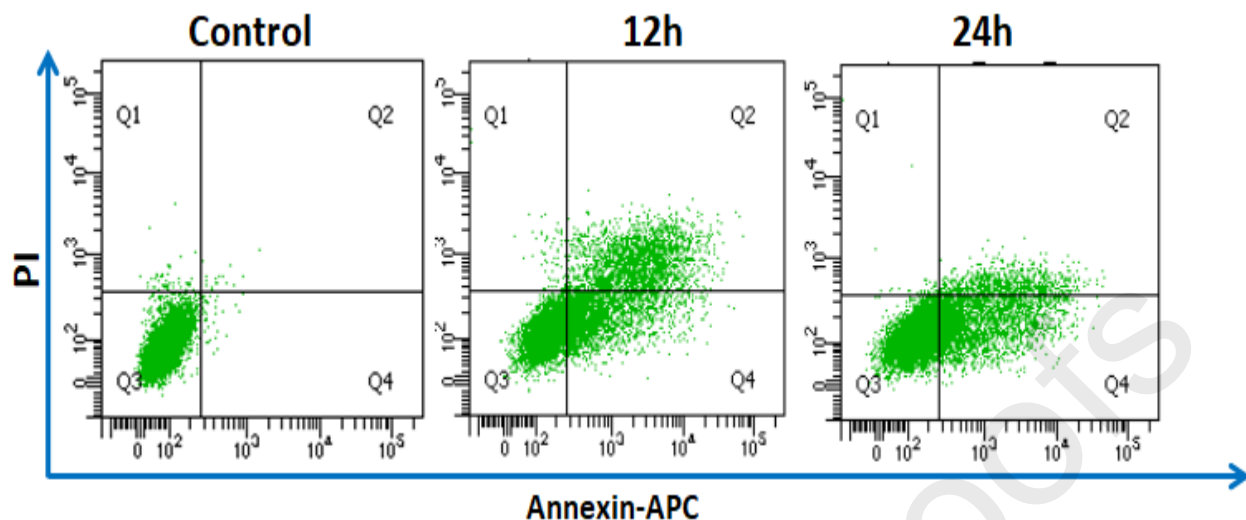


**Fig. 4** Determination of apoptosis/necrosis after treatment of 9  $\mu\text{M}$  complex **1** against human colorectal HCT 116 cancer cell lines.

### 3.5. Determination of intracellular ROS (iROS)

There are several reports confirmed that Apoptosis is directly dependent on Reactive Oxygen Species (ROS) [61,62]. The total ROS generation has been quantified after treatment of 9  $\mu\text{M}$  complex **1** (Fig. 5) by using a cell permeable dye, DCFH-DA.

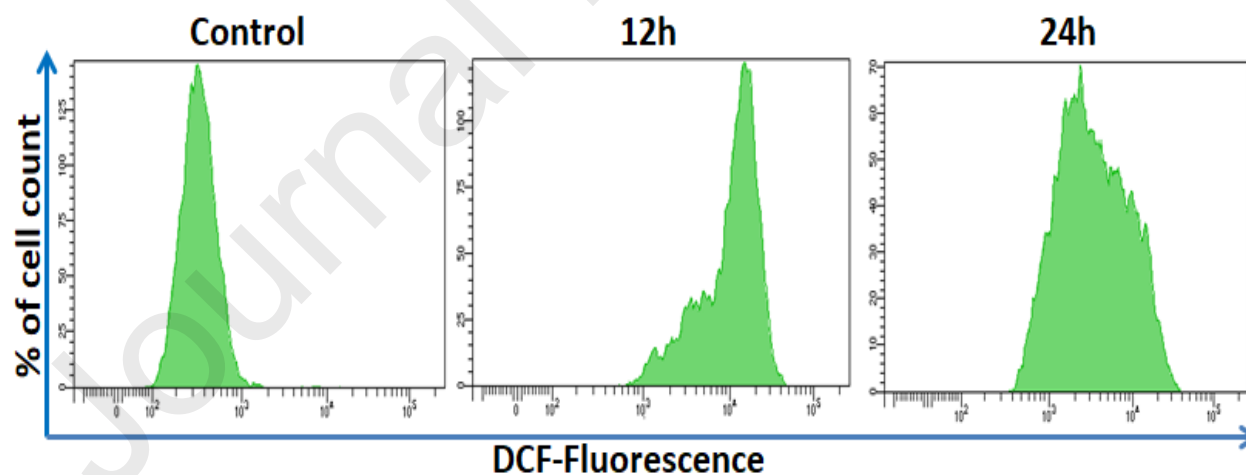


**Fig. 5** Determination of iROS after treatment of 9  $\mu\text{M}$  complex **1** against human colorectal HCT 116 cancer cell lines.

In this flow cytometric data, complex **1** treated with HCT-116 cells showed an overproduction of ROS by markedly increased DCF fluorescence reflecting the increased DCF +Ve cells when

treated for 12 and 24 h and compared with the control cells. This data confirmed that the cell death of HCT 116 was occurring by ROS dependent apoptosis [63].

### 3.6. Assessment of protein expression

Bax acts upstream of increased Reactive Oxygen Species (ROS) production [64]. There are also some reports which cleared that Bax activation are essential for cytochrome *c* release from Mitochondria during apoptosis [65]. Bax and Cytochrome *c* are also two key pro-apoptotic marker for apoptosis [66]. So, we have tried to establish the relation of Bax and Cytochrome *c* release after treatment of 9  $\mu$ M complex 1 in presence of MitoTracker Red and Nuclear stainer DAPI (Fig. 6).

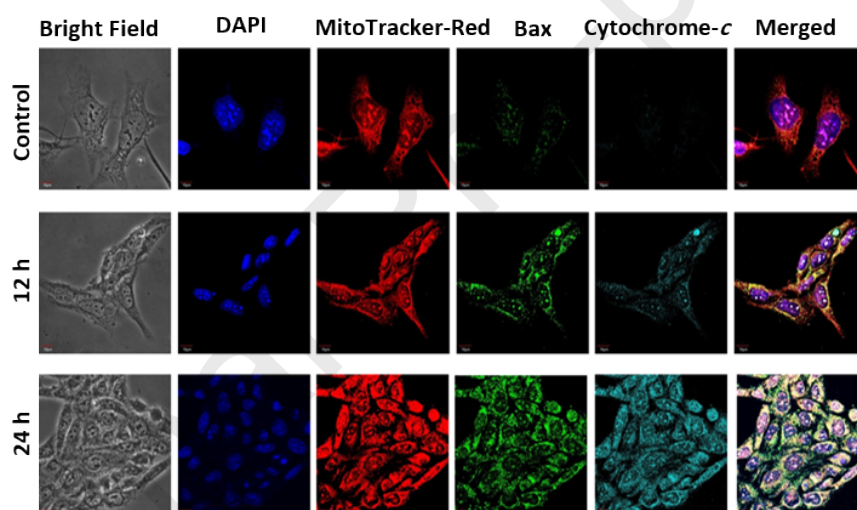


**Fig. 6** Expression of Bax and Cytochrome *c* after treatment of 9  $\mu$ M complex 1 in presence of DAPI and MitoTracker-Red on human colorectal HCT 116 cancer cell lines.

The expression of Bax and Cytochrome *c* has been increased after treatment of complex 1 time dependently. The final apoptotic fate was determined by the activity of caspase-9 and caspase-3 [67] (Fig. 7), which was simultaneously enhanced with the treatment of complex 1. Simultaneously, scratch assay was performed for measuring cell proliferation after 12h of

complex 1 treatment. The microscopic images (Fig. S4) revealed that there was no such cell proliferation after 12h of complex 1 treatment.

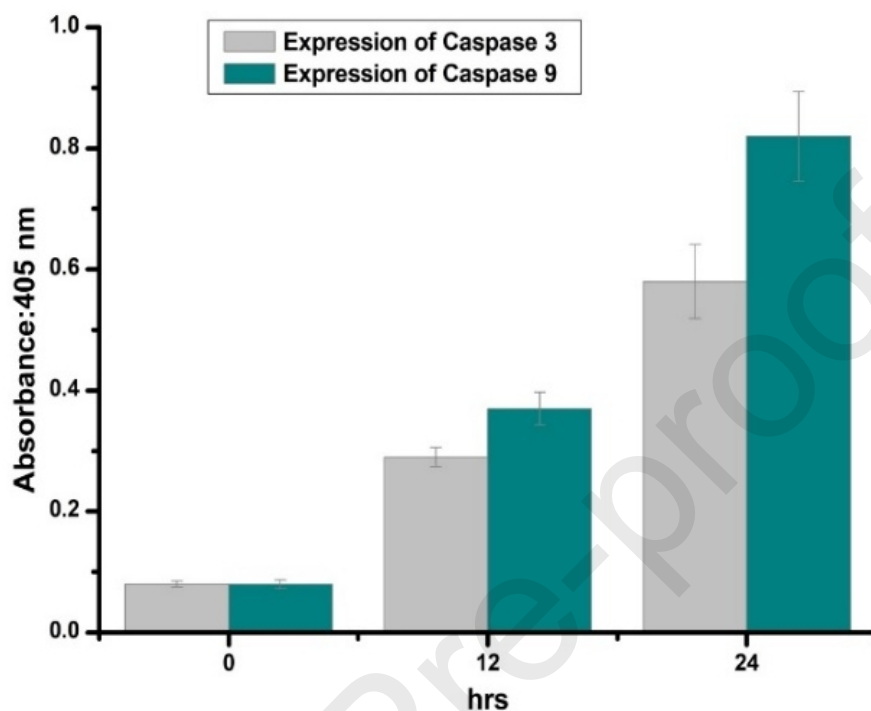
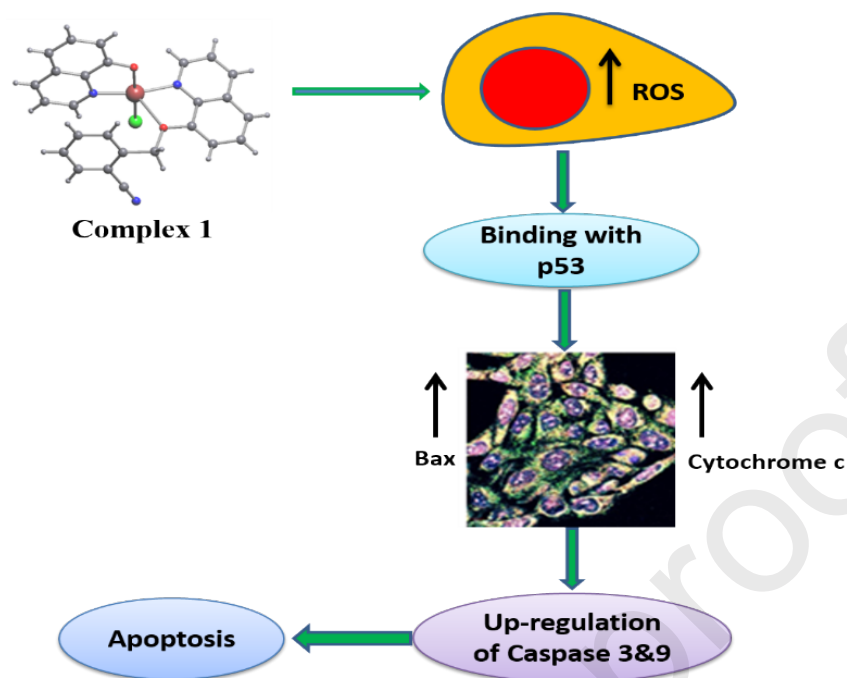


**Fig.7** Expression of caspase 3 and 9 after treatment of 9  $\mu$ M complex 1.

The result summarily confirms that complex 1 mediated apoptosis might be regulated through ROS driven mitochondrial pathway of apoptosis. Thus, complex 1 induces mitochondrial dependence apoptosis through the modulation of pro- and anti-apoptotic proteins (Scheme 2).



**Scheme 2.** Schematic representation of the overall events of apoptotic pathway induced by complex **1**. The  $\uparrow$  arrows indicate the up-regulation of that particular marker induces apoptosis in cancer cells.

### 3.7. Catalytic activity

The catecholase-like activity of complex **1** was monitored using catechol as the substrates for the identification of complex **1** as functional model for metalloenzymes. Copper(II) complex containing 8-hydroxyquinoline and pyrazine-2-carboxylic acid also serves as an efficient heterogeneous catalysts for the elimination of dye in aqueous solution with  $\text{H}_2\text{O}_2$  in a short time [68]. To date, many mono or binuclear copper complexes derived from oxygen and nitrogen donating ligands which exhibited potential catalytic activity towards the conversion of 3,5-DTBC to 3,5-DTBQ in presence of molecular oxygen [69]. The catecholase mimicking activity of the complex **1** (0.0001M) was evaluated using 3,5-DTBC (3,5-di-tert-butylcatechol) (0.01M) as a substrate under aerobic conditions. The reactions were carried out in dioxygen saturated ethanol at 25 °C under aerobic conditions and their absorption spectra were recorded at time

interval of every five minutes. The substrate 3,5-DTBC has low redox potential that facilitated its oxidation, and the resulting product, 3,5-DTBQ has exhibited a characteristic strong absorption maximum at ca. 393 nm ( $\epsilon = 1900 \text{ M}^{-1}\text{cm}^{-1}$ ) [69]. The time dependent spectral changes of the complex **1** was followed spectrophotometrically at 393 nm for about 100 min at regular time interval of 5 min upon the addition of 3,5-DTBC (Fig. 8). The increase in absorbance at monitoring wavelength clearly demonstrated that the complex **1** was efficiently and effectively oxidizing substrate 3,5-DTBC to 3,5-DTBQ.

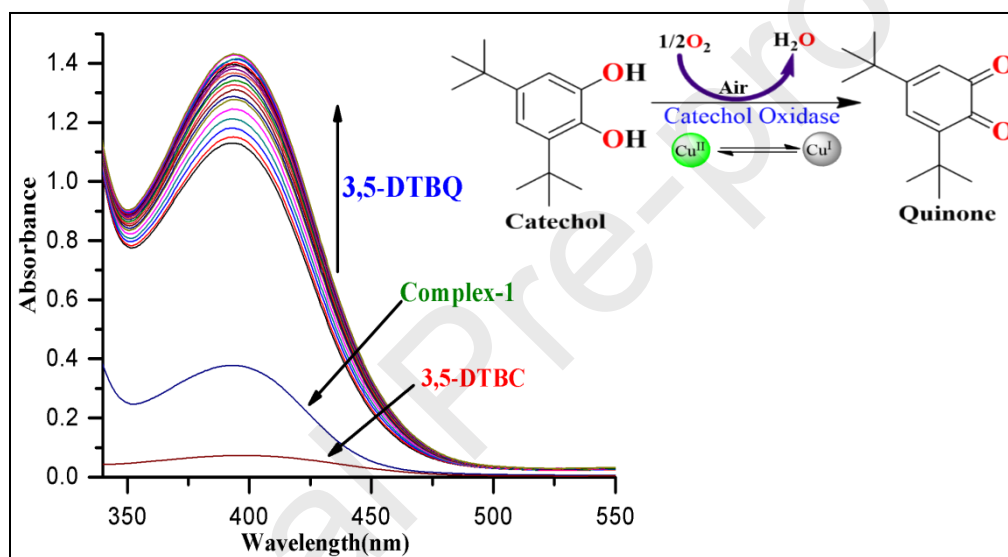


**Fig. 8.** Uv-vis spectra recorded in the presence of complex **1** upon addition of 3,5-DTBC at a regular time interval of 5min.

### 3.8. Kinetic study of catechol oxidation

From the above experimental results, it was observed that complex **1** has ability to catalyze the oxidation of substrate 3,5-DTBC. Therefore, a detailed quantitative kinetic study model of complex **1** was conducted to further elucidate its catalytic efficiency towards 3,5-DTBC in dioxygen saturated ethanol under experimental conditions. Solutions of the complex **1** (0.0001 M) was treated with incremental addition of 3,5-DTBC (0.0001 M to 0.001 M), and their

absorption spectra were recorded. An analysis of the data based on the method of initial rate, kinetics determination was applied following the conversion of 3,5-DTBC to the increase in oxidized product 3, 5-DTBQ at 393 nm every five minutes. The average value of rate constant of reaction for the complex **1** showed zero order at high concentration of 3,5-DTBC substrate but at low concentration, average rate constant follows the first order reaction. The Michaelis-Menten model, originally developed for enzyme kinetics may be appropriate for this conversion also.

$$V = \frac{V_{max}[S]}{K_M + [S]}$$

Where  $V$  = initial rate,  $[S]$  = concentration of 3,5-DTBC substrate;  $K_M = (k_2+k_3/K_1)$ , Michaelis-Menten constant and  $V_{max}$  = maximum initial rate accomplished for a particular concentration of complex **1** in the presence of excess amount of 3,5-DTBC (Fig. 9a). Mathematically, the Michaelis-Menten equation can be transformed into another form which is more useful in data plotting. Taking the reciprocal of both sides, the above equation transformed to the well-known Lineweaver-Burk equation;

$$\frac{1}{V} = \frac{K_M}{V_{max}} \times \frac{1}{[S]} + \frac{1}{V_{max}}$$

The value of Michaelis-Menten binding constant ( $K_M$ ), maximum velocity ( $V_{max}$ ), and rate constant for dissociation of substrate (i.e. turnover number  $K_{cat}$ ) were calculated from the plot of  $1/V$  vs  $1/[S]$  (Fig. 9b), also known as Lineweaver-Burk plot. A linear relation between the concentration of the complex **1** and its initial rate of the oxidation, confirming a first-order dependence on the complex concentration and the calculated kinetic parameters obtained were  $k_{cat}=1.03 \times 10^2 \text{ h}^{-1}$ ,  $K_M = 0.0209 \text{ M}$  and  $V_{max}= 2.87 \times 10^{-2} \text{ M min}^{-1}$ . Moreover, the catecholase mimics activity of the complex **1** was compared to previously reported metal complexes (Table 4) [70–75].

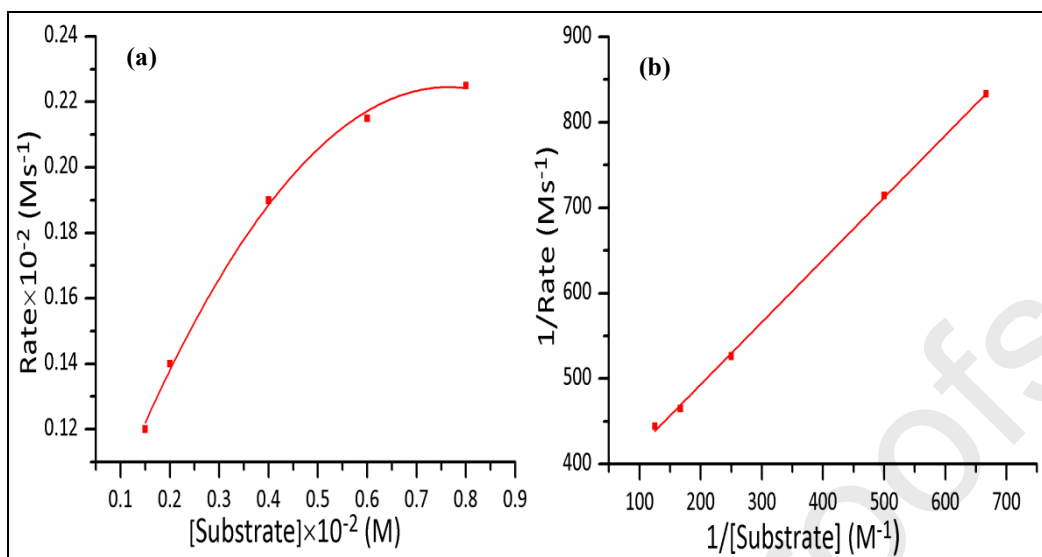
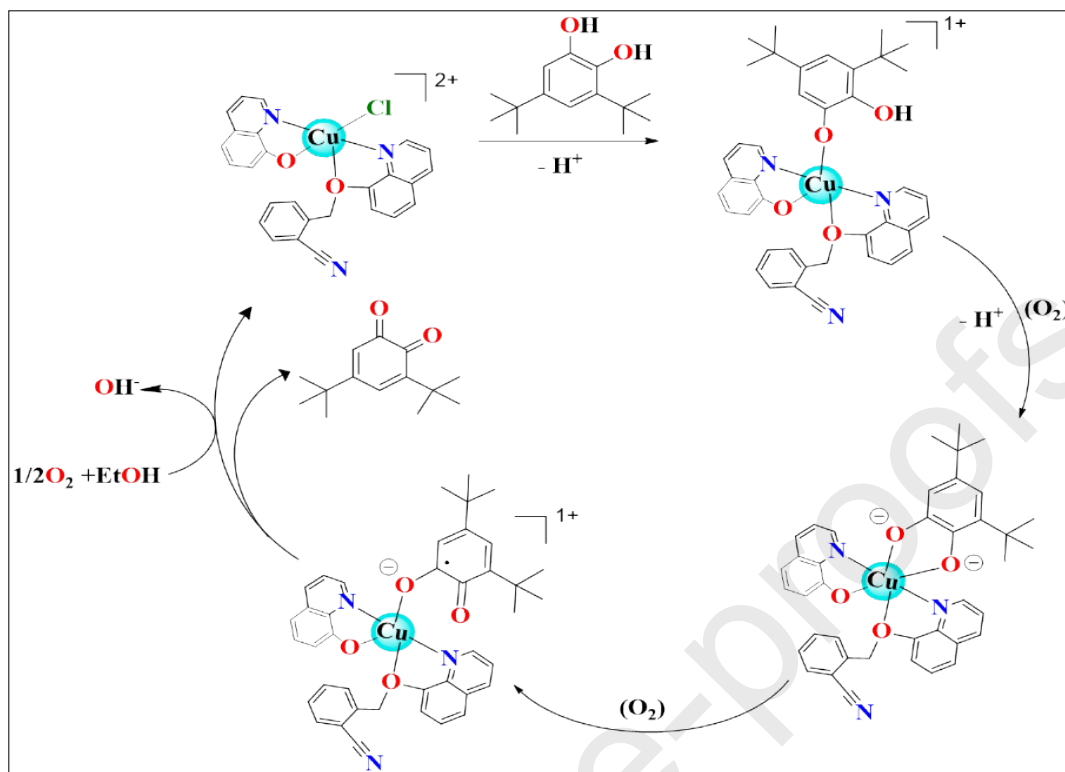


**Fig.9** Plot of (a) rate vs substrate concentration and (b) Lineweaver-Burk plot of complex **1**.

**Table 4.** Catalytic turnover number ( $k_{\text{cat}}$ ) for the oxidation of DTBC by complex **1** and previously known metal(II) complexes.

Metal(II) complexes	$k_{\text{cat}}(\text{h}^{-1})$	Ref.
$[\text{Cu}_2(\text{H}_2\text{L}^{22})(\text{OH})(\text{H}_2\text{O})(\text{NO}_3)](\text{NO}_3)_3 \cdot 2\text{H}_2\text{O}$	$3.24 \times 10^4$	[70]
$[\text{Cu}(\text{HL}^{14})(\text{H}_2\text{O})(\text{NO}_3)]_2 \cdot (\text{NO}_3)_2 \cdot 2\text{H}_2\text{O}$	$1.44 \times 10^4$	[70]
$[\text{Cu}(\text{L}^{11})(\text{H}_2\text{O})(\text{NO}_3)]_2$	$1.08 \times 10^4$	[70]
$[\text{Cu}_2(\text{L}^{23})(\text{OH})(\text{H}_2\text{O})_2](\text{NO}_3)_2$	$1.44 \times 10^4$	[70]
$[\text{Cu}_2(\text{L}^{21})(\text{N}_3)_3]$	$2.88 \times 10^4$	[70]
$[\text{Cu}_2(\text{L})(\mu\text{-OH})(\text{H}_2\text{O})(\text{ClO}_4)_2]$	$0.76 \times 10^2$	[71]
$[\text{Cu}_2(\text{L}^{22})_2(\text{OAc})_2] \cdot \text{H}_2\text{O}$	$102 \times 10^4$	[72]
$[\text{Co}(\text{L})_2(\text{H}_2\text{O})_2]$	$1.68 \times 10^2$	[73]
$[\text{Ni}_2(\text{L}^1)_2(\text{NCS})_2]$	$64.1 \pm 4.1$	[74]
$[\text{Ni}_2(\text{L}^2)_2(\text{NCS})_2]$	$51.1 \pm 6.2$	[74]
$[\text{Ni}_2(\text{L}^3)_2(\text{NCS})_2]$	$81.7 \pm 4.7$	[74]
$\{[\text{Cu}^{\text{I}}(\text{CN})(\text{phen})_2\text{Cu}^{\text{II}}(\text{CN})_2(\text{phen})] \cdot 5\text{H}_2\text{O}\}$	$1.88 \times 10^3$	[75]
$[\text{Cu}(\text{qmbn})(\text{q})(\text{Cl})]$	$1.03 \times 10^2$	this work



**Scheme 3.** A plausible mechanism for catecholase like activity promoted by complex **1** involving catalytic oxidation of 3,5-DTBC to 3,5-DTBQ.

A plausible mechanism for the aerobic oxidation of catechol to quinone promoted by complex **1** is depicted in Scheme 3. In the first step of the catalytic cycle, the complex **1** successfully reacted with the catechol leads to the generation of radical intermediate Cu(I)-semiquinone complex followed by reduction of Cu(II)-Cu(I). Subsequently, Cu(I)-semiquinone radical intermediate get oxidized in the presence of dioxygen leading to the re-oxidation of Cu(I) to Cu(II) and the reduction of dioxygen. Notably, it may be attributed that Cu(II)-semiquinone radical species either get oxidized by  $O_2$  to quinone or disproportionated to quinone followed by further oxidation of the copper ions.

### 3.9. Molecular docking

To explore the potential binding modes of the complex **1** and protein kinase (Akt), molecular docking was performed to understand the experimental findings as described above. The target

receptor human Akt kinase (PDB: 3MVH) has been chosen to probe the possible molecular mechanism of interactions with complex **1**. It is well-known that Akt kinases are among the most thoroughly studied targets for targeted cancer therapeutic agents, due to their close resemblance with multiple cellular signaling pathways such as glucose metabolism, apoptosis, cell proliferation, transcription, and cell migration. Based on *in silico* results, the docked pose analysis results showed that complex **1** recognizes the binding pocket that was provided by the target receptor (Fig. 10a). Furthermore, several amino acid residues directly interacted with molecule, as lowest energy docked pose of the complex **1** displayed that planar aromatic part of the complex develops arene-arene interactions with aromatic ring of Tyrosine residues (Tyr175 & Tyr-176) as indicated by 2D ligplot (Fig. 10b).

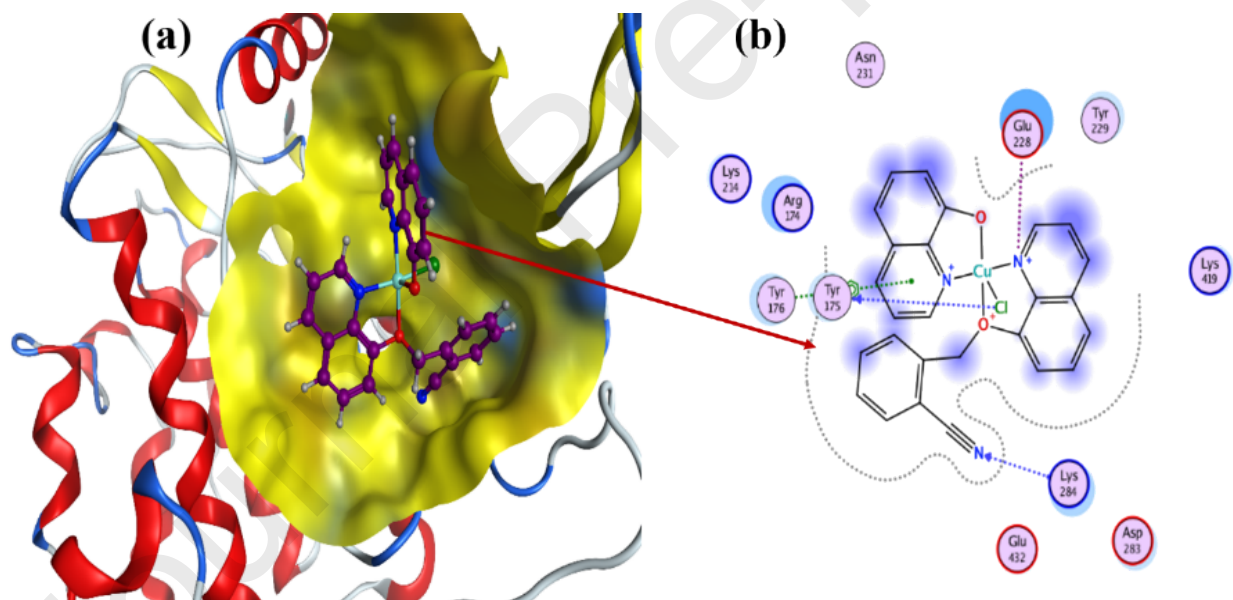


**Fig. 10**(a) Molecular docking pose of complex **1** with human Akt kinase (PDB ID: 3MVH) and (b) 2D ligplots which show interactions of complex **1** with base pairs of Akt receptor.

The H-bonding interactions develop between  $-N$  atom of complex with H atom of Glutamic acid (Glu228) and Lysine (Lys284). Other two interactions include electrostatic interaction of Cl-atom of complex with H-atom of Tyr-175. Dotted lines around molecule indicate hydrophobic

interactions with Akt receptor. Greater number of interactions are responsible for high binding constant ( $K_b = 2.52 \times 10^4 \text{ M}^{-1}$ ) and higher spontaneity of complex formation with greater negative value of free energy ( $\Delta G = -25.11 \text{ kJ mol}^{-1}$ ). The model might serve as a rational basis for possible design of novel anticancer drugs targeting active site of human Akt kinase.

#### 4. Conclusion

Herein, we have designed and synthesized a new copper(II) complex  $[\text{Cu}(\text{qmbn})(\text{q})(\text{Cl})]$  (**1**) as potential chemotherapeutic agent. Structural elucidation of the complex **1** was done by various analytical (elemental analysis, TGA and XRD) and spectroscopic techniques (IR and Uv-vis). *In vitro* cytotoxicity of the complex **1** was evaluated on the human colon cancer cell line (HCT116) which implicated that more than 50% cells were viable at  $9.82 \mu\text{M}$  after 12h of treatment. The outcomes of flow cytometric and fluorescence microscopic analysis were in concordance with the results of MTT assay which showed a time-dependent increase in the number of apoptotic cells. The mitochondrial pathway plays an important role in inducing cell apoptosis based on the results of up-regulated expression of Bax and Cytochrome-*c* which ultimately triggers the caspase 3/9 protein activation and ultimately lead to apoptosis. Interestingly, complex **1** exhibited significant catecholase like activity  $k_{\text{cat}} = 1.03 \times 10^2 \text{ h}^{-1}$ . Furthermore, molecular docking results revealed that the complex **1** binds to the active site of protein kinase (Akt), which plays a key role in multiple cellular processes such as apoptosis, cell proliferation, and cell migration.

#### Acknowledgements

The Department of Applied Chemistry, Faculty of Engineering and Technology, Aligarh Muslim University, UP, India, and Researchers Supporting Project number (RSP-2020/288), King Saud University, Riyadh, Saudi Arabia are gratefully acknowledged for financial support and

laboratory facilities. UGC Start-up grant and TEQIP-III, ZHCET, Aligarh Muslim University, is thanked for extensive help to procure chemicals.

### Supporting Information

CCDC 2003694 contains the supplementary crystallographic data for complex **1**. It data can be obtained free of charge via <http://www.ccdc.cam.ac.uk/conts/retrieving.html>, or from the Cambridge Crystallographic Data Centre, 12 Union Road, Cambridge CB2 1EZ, UK; fax: (+44) 1223-336-033; or e-mail: [deposit@ccdc.cam.ac.uk](mailto:deposit@ccdc.cam.ac.uk). Table for selected bond lengths and bond angles, IR, TGA and PXRD and scratch assay are appended.

### Authorship Contributions

The manuscript was written through contributions of all authors. All authors have given approval to the final version of the manuscript.

### Notes

There is no conflict of interest to declare.

### References

- [1] I. Ewing, J.J. Hurley, E. Josephides, A. Millar, The molecular genetics of colorectal cancer, *Frontline Gastroenterol.* 5 (2014) 26–30. <https://doi.org/10.1136/flgastro-2013-100329>.
- [2] P. Rawla, T. Sunkara, A. Barsouk, Epidemiology of colorectal cancer: incidence, mortality, survival, and risk factors, *Gastroenterol. Rev.* 14 (2019) 89–103. <https://doi.org/10.5114/pg.2018.81072>.
- [3] H. Brenner, C. Chen, The colorectal cancer epidemic: challenges and opportunities for primary, secondary and tertiary prevention, *Br. J. Cancer.* 119 (2018) 785–792. <https://doi.org/10.1038/s41416-018-0264-x>.
- [4] D.A. Bardi, M.F. Halabi, P. Hassandarvish, E. Rouhollahi, M. Paydar, S.Z. Moghadamtousi, N.S. Al-Wajeeh, A. Ablat, N.A. Abdullah, M.A. Abdulla, *Andrographis paniculata* Leaf Extract Prevents Thioacetamide-Induced Liver Cirrhosis in Rats, *PLoS One.* 9 (2014) e109424. <https://doi.org/10.1371/journal.pone.0109424>.

- [5] B. Hu, E. Elinav, S. Huber, C.J. Booth, T. Strowig, C. Jin, S.C. Eisenbarth, R.A. Flavell, Inflammation-induced tumorigenesis in the colon is regulated by caspase-1 and NLRC4, *Proc. Natl. Acad. Sci.* 107 (2010) 21635–21640. <https://doi.org/10.1073/pnas.1016814108>.
- [6] A.I. Matos, B. Carreira, C. Peres, L.I.F. Moura, J. Conriot, T. Fourniols, A. Scomparin, Á. Martínez-Barriocanal, D. Arango, J.P. Conde, V. Pr eat, R. Satchi-Fainaro, H.F. Florindo, Nanotechnology is an important strategy for combinational innovative chemo-immunotherapies against colorectal cancer, *J. Control. Release.* 307 (2019) 108–138. <https://doi.org/10.1016/j.jconrel.2019.06.017>.
- [7] S.J. Allison, D. Cooke, F.S. Davidson, P.I.P. Elliott, R.A. Faulkner, H.B.S. Griffiths, O.J. Harper, O. Hussain, P.J. Owen-Lynch, R.M. Phillips, C.R. Rice, S.L. Shepherd, R.T. Wheelhouse, Ruthenium-Containing Linear Helicates and Mesocates with Tuneable p53-Selective Cytotoxicity in Colorectal Cancer Cells, *Angew. Chemie.* 130 (2018) 9947–9952. <https://doi.org/10.1002/ange.201805510>.
- [8] R. Yehia, S. Saleh, H. El Abhar, A.S. Saad, M. Schaalaa, L-Carnosine protects against Oxaliplatin-induced peripheral neuropathy in colorectal cancer patients: A perspective on targeting Nrf-2 and NF- $\kappa$ B pathways, *Toxicol. Appl. Pharmacol.* 365 (2019) 41–50. <https://doi.org/10.1016/j.taap.2018.12.015>.
- [9] C.J. Brown, S. Lain, C.S. Verma, A.R. Fersht, D.P. Lane, Awakening guardian angels: drugging the p53 pathway, *Nat. Rev. Cancer.* 9 (2009) 862–873. <https://doi.org/10.1038/nrc2763>.
- [10] B.S. Tan, K.H. Tiong, H.L. Choo, F. Fei-Lei Chung, L.-W. Hii, S.H. Tan, I.K. Yap, S. Pani, N.T. Khor, S.F. Wong, R. Rosli, S.-K. Cheong, C.-O. Leong, Mutant p53-R273H mediates cancer cell survival and anoikis resistance through AKT-dependent suppression of BCL2-modifying factor (BMF), *Cell Death Dis.* 6 (2015) e1826–e1826. <https://doi.org/10.1038/cddis.2015.191>.
- [11] Y. Haupt, R. Maya, A. Kazaz, M. Oren, Mdm2 promotes the rapid degradation of p53, *Nature.* 387 (1997) 296–299. <https://doi.org/10.1038/387296a0>.
- [12] S. You, W. Rui, S. Chen, H. Chen, X. Liu, J. Huang, H. Chen, Process of immunogenic cell death caused by disulfiram as the anti-colorectal cancer candidate, *Biochem. Biophys. Res. Commun.* 513 (2019) 891–897. <https://doi.org/10.1016/j.bbrc.2019.03.192>.

- [13] A.C. Joerger, A.R. Fersht, The p53 Pathway: Origins, Inactivation in Cancer, and Emerging Therapeutic Approaches, *Annu. Rev. Biochem.* 85 (2016) 375–404. <https://doi.org/10.1146/annurev-biochem-060815-014710>.
- [14] L.M. Beaver, T.-W. Yu, E.I. Sokolowski, D.E. Williams, R.H. Dashwood, E. Ho, 3,3'-Diindolylmethane, but not indole-3-carbinol, inhibits histone deacetylase activity in prostate cancer cells, *Toxicol. Appl. Pharmacol.* 263 (2012) 345–351. <https://doi.org/10.1016/j.taap.2012.07.007>.
- [15] N.B. Janakiram, V.E. Steele, C. V. Rao, Estrogen Receptor- as a Potential Target for Colon Cancer Prevention: Chemoprevention of Azoxymethane-Induced Colon Carcinogenesis by Raloxifene in F344 Rats, *Cancer Prev. Res.* 2 (2009) 52–59. <https://doi.org/10.1158/1940-6207.CAPR-08-0140>.
- [16] Z.-Y. Ma, X. Qiao, C.-Z. Xie, J. Shao, J.-Y. Xu, Z.-Y. Qiang, J.-S. Lou, Activities of a novel Schiff Base copper(II) complex on growth inhibition and apoptosis induction toward MCF-7 human breast cancer cells via mitochondrial pathway, *J. Inorg. Biochem.* 117 (2012) 1–9. <https://doi.org/10.1016/j.jinorgbio.2012.08.007>.
- [17] S. Jiang, H. Ni, F. Liu, S. Gu, P. Yu, Y. Gou, Binuclear Schiff base copper(II) complexes: Syntheses, crystal structures, HSA interaction and anti-cancer properties, *Inorganica Chim. Acta.* 499 (2020) 119186. <https://doi.org/10.1016/j.ica.2019.119186>.
- [18] H. Mutlu Gençkal, M. Erkisa, P. Alper, S. Sahin, E. Ulukaya, F. Ari, Mixed ligand complexes of Co(II), Ni(II) and Cu(II) with quercetin and diimine ligands: synthesis, characterization, anti-cancer and anti-oxidant activity, *J. Biol. Inorg. Chem.* 25 (2020) 161–177. <https://doi.org/10.1007/s00775-019-01749-z>.
- [19] J.-L. Qin, W.-Y. Shen, Z.-F. Chen, L.-F. Zhao, Q.-P. Qin, Y.-C. Yu, H. Liang, Oxoaporphine Metal Complexes (Co<sup>II</sup>, Ni<sup>II</sup>, Zn<sup>II</sup>) with High Antitumor Activity by Inducing Mitochondria-Mediated Apoptosis and S-phase Arrest in HepG2, *Sci. Rep.* 7 (2017) 46056. <https://doi.org/10.1038/srep46056>.
- [20] N. Kordestani, H.A. Rudbari, A.R. Fernandes, L.R. Raposo, P. V. Baptista, D. Ferreira, G. Bruno, G. Bella, R. Scopelliti, J.D. Braun, D.E. Herbert, O. Blacque, Antiproliferative Activities of Diimine-Based Mixed Ligand Copper(II) Complexes, *ACS Comb. Sci.* 22 (2020) 89–99. <https://doi.org/10.1021/acscombsci.9b00202>.

- [21] C.H. Ng, S.M. Kong, Y.L. Tiong, M.J. Maah, N. Sukram, M. Ahmad, A.S.B. Khoo, Selective anticancer copper(II)-mixed ligand complexes: targeting of ROS and proteasomes, *Metallomics*. 6 (2014) 892–906. <https://doi.org/10.1039/C3MT00276D>.
- [22] P. Bhanja, S. Mishra, K. Manna, A. Mallick, K. Das Saha, A. Bhaumik, Covalent Organic Framework Material Bearing Phloroglucinol Building Units as a Potent Anticancer Agent, *Appl. Mater. Interfaces*. 9 (2017) 31411–31423. <https://doi.org/10.1021/acsami.7b07343>.
- [23] M. Gobec, J. Kljun, I. Sosič, I. Mlinarič-Raščan, M. Uršič, S. Gobec, I. Turel, Structural characterization and biological evaluation of a clioquinol–ruthenium complex with copper-independent antileukaemic activity, *Dalt. Trans.* 43 (2014) 9045–9051. <https://doi.org/10.1039/C4DT00463A>.
- [24] R. Musiol, J. Jampilek, V. Buchta, L. Silva, H. Niedbala, B. Podeszwa, A. Palka, K. Majerz-Maniecka, B. Oleksyn, J. Polanski, Antifungal properties of new series of quinoline derivatives, *Bioorg. Med. Chem.* 14 (2006) 3592–3598. <https://doi.org/10.1016/j.bmc.2006.01.016>.
- [25] P. Palit, P. Paira, A. Hazra, S. Banerjee, A. Das Gupta, S.G. Dastidar, N.B. Mondal, Phase transfer catalyzed synthesis of bis-quinolines: Antileishmanial activity in experimental visceral leishmaniasis and in vitro antibacterial evaluation, *Eur. J. Med. Chem.* 44 (2009) 845–853. <https://doi.org/10.1016/j.ejmech.2008.04.014>.
- [26] S.H. Chan, C.H. Chui, S.W. Chan, S.H.L. Kok, D. Chan, M.Y.T. Tsoi, P.H.M. Leung, A.K.Y. Lam, A.S.C. Chan, K.H. Lam, J.C.O. Tang, Synthesis of 8-Hydroxyquinoline Derivatives as Novel Antitumor Agents, *ACS Med. Chem. Lett.* 4 (2013) 170–174. <https://doi.org/10.1021/ml300238z>.
- [27] F. Zouhiri, M. Danet, C. Bénard, M. Normand-Bayle, J.-F. Mouscadet, H. Leh, C. Marie Thomas, G. Mbemba, J. D'Angelo, D. Desmaële, HIV-1 replication inhibitors of the styrylquinoline class: introduction of an additional carboxyl group at the C-5 position of the quinoline, *Tetrahedron Lett.* 46 (2005) 2201–2205. <https://doi.org/10.1016/j.tetlet.2005.02.033>.
- [28] M. Krawczyk, G. Pastuch-Gawolek, A. Pluta, K. Erfurt, A. Domiński, P. Kurcok, 8-Hydroxyquinoline Glycoconjugates: Modifications in the Linker Structure and Their Effect on the Cytotoxicity of the Obtained Compounds, *Molecules*. 24 (2019) 4181. <https://doi.org/10.3390/molecules24224181>.

- [29] L.M. Guamán Ortiz, M. Tillhon, M. Parks, I. Dutto, E. Prospero, M. Savio, A.G. Arcamone, F. Buzzetti, P. Lombardi, A.I. Scovassi, Multiple Effects of Berberine Derivatives on Colon Cancer Cells, *Biomed Res. Int.* 2014 (2014) 1–12. <https://doi.org/10.1155/2014/924585>.
- [30] Y. Ai, Y.-J. Liang, J.-C. Liu, H.-W. He, Y. Chen, C. Tang, G.-Z. Yang, L.-W. Fu, Synthesis and in vitro antiproliferative evaluation of pyrimido[5,4-c]quinoline-4-(3H)-one derivatives, *Eur. J. Med. Chem.* 47 (2012) 206–213. <https://doi.org/10.1016/j.ejmech.2011.10.044>.
- [31] B. Rosenberg, L.V. Camp, T. Krigas, Inhibition of Cell Division in *Escherichia coli* by Electrolysis Products from a Platinum Electrode, *Nature*. 205 (1965) 698–699. <https://doi.org/10.1038/205698a0>.
- [32] I. Kostova, Platinum Complexes as Anticancer Agents, *Recent Pat. Anticancer. Drug Discov.* 1 (2006) 1–22. <https://doi.org/10.2174/157489206775246458>.
- [33] M.J. Hannon, Metal-based anticancer drugs: From a past anchored in platinum chemistry to a post-genomic future of diverse chemistry and biology, *Pure Appl. Chem.* 79 (2007) 2243–2261. <https://doi.org/10.1351/pac200779122243>.
- [34] G. Psomas, D.P. Kessissoglou, Quinolones and non-steroidal anti-inflammatory drugs interacting with copper(II), nickel(II), cobalt(II) and zinc(II): structural features, biological evaluation and perspectives, *Dalt. Trans.* 42 (2013) 6252–6276. <https://doi.org/10.1039/c3dt50268f>.
- [35] D. Mahendiran, R.S. Kumar, V. Viswanathan, D. Velmurugan, A.K. Rahiman, Targeting of DNA molecules, BSA/c-Met tyrosine kinase receptors and anti-proliferative activity of bis(terpyridine)copper(II) complexes, *Dalt. Trans.* 45 (2016) 7794–7814. <https://doi.org/10.1039/C5DT03831F>.
- [36] B.S. Mendiguchia, I. Aiello, A. Crispini, Zn(II) and Cu(II) complexes containing bioactive O,O-chelated ligands: homoleptic and heteroleptic metal-based biomolecules, *Dalt. Trans.* 44 (2015) 9321–9334. <https://doi.org/10.1039/C5DT00817D>.
- [37] D.G. Barceloux, D. Barceloux, Copper, *J. Toxicol. Clin. Toxicol.* 37 (1999) 217–230. <https://doi.org/10.1081/CLT-100102421>.
- [38] S. Ishida, F. McCormick, K. Smith-McCune, D. Hanahan, Enhancing Tumor-Specific Uptake of the Anticancer Drug Cisplatin with a Copper Chelator, *Cancer Cell*. 17 (2010)

- 574–583. <https://doi.org/10.1016/j.ccr.2010.04.011>.
- [39] R.A. Steiner, D. Foreman, H.X. Lin, B.K. Carney, K.M. Fox, L. Cassimeris, J.M. Tanski, L.A. Tyler, Synthesis, characterization, crystal structures and biological activity of set of Cu(II) benzothiazole complexes: Artificial nucleases with cytotoxic activities, *J. Inorg. Biochem.* 137 (2014) 1–11. <https://doi.org/10.1016/j.jinorgbio.2014.04.002>.
- [40] S. Sarkar, T. Mukherjee, S. Sen, E. Zangrando, P. Chattopadhyay, Copper(II) complex of in situ formed 5-(2-pyridyl)-1,3,4-triazole through C–S bond cleavage in 1,2-bis(2-pyridylmethylthio)-bis-ethylsulphide: Synthesis, structural characterization and DNA binding study, *J. Mol. Struct.* 980 (2010) 117–123. <https://doi.org/10.1016/j.molstruc.2010.07.002>.
- [41] International Tables for X-Ray Crystallography, Vol. III, Kynoch Press, Birmingham, England, 1952, pp. 257–269.
- [42] O. V. Dolomanov, L.J. Bourhis, R.J. Gildea, J.A.K. Howard, H. Puschmann, OLEX2 : a complete structure solution, refinement and analysis program, *J. Appl. Crystallogr.* 42 (2009) 339–341. <https://doi.org/10.1107/S0021889808042726>.
- [43] L.J. Bourhis, O. V. Dolomanov, R.J. Gildea, J.A.K. Howard, H. Puschmann, The anatomy of a comprehensive constrained, restrained refinement program for the modern computing environment – Olex2 dissected, *Acta Crystallogr. Sect. A Found. Adv.* 71 (2015) 59–75. <https://doi.org/10.1107/S2053273314022207>.
- [44] K.N. Tiwari, J.-P. Monserrat, A. Hequet, C. Ganem-Elbaz, T. Cresteil, G. Jaouen, A. Vessières, E.A. Hillard, C. Jolivald, In vitro inhibitory properties of ferrocene-substituted chalcones and aurones on bacterial and human cell cultures, *Dalt. Trans.* 41 (2012) 6451–6457. <https://doi.org/10.1039/c2dt12180h>.
- [45] R. Nandi, S. Mishra, T.K. Maji, K. Manna, P. Kar, S. Banerjee, S. Dutta, S.K. Sharma, P. Lemmens, K. Das Saha, S.K. Pal, A novel nanohybrid for cancer theranostics: folate sensitized Fe<sub>2</sub>O<sub>3</sub> nanoparticles for colorectal cancer diagnosis and photodynamic therapy, *J. Mater. Chem. B.* 5 (2017) 3927–3939. <https://doi.org/10.1039/C6TB03292C>.
- [46] A. Datta, S. Mishra, K. Manna, K. Das Saha, S. Mukherjee, S. Roy, Pro-Oxidant Therapeutic Activities of Cerium Oxide Nanoparticles in Colorectal Carcinoma Cells, *ACS Omega.* 5 (2020) 9714–9723. <https://doi.org/10.1021/acsomega.9b04006>.
- [47] M. Redza-Dutordoir, D.A. Averill-Bates, Activation of apoptosis signalling pathways by

- reactive oxygen species, *Biochim. Biophys. Acta - Mol. Cell Res.* 1863 (2016) 2977–2992. <https://doi.org/10.1016/j.bbamcr.2016.09.012>.
- [48] A. Mukherjee, S. Mishra, N.K. Kotla, K. Manna, S. Roy, B. Kundu, D. Bhattacharya, K. Das Saha, A. Talukdar, Semisynthetic Quercetin Derivatives with Potent Antitumor Activity in Colon Carcinoma, *ACS Omega*. 4 (2019) 7285–7298. <https://doi.org/10.1021/acsomega.9b00143>.
- [49] S. Chatterjee, S. Ghosh, S. Mishra, K. Das Saha, B. Banerji, K. Chattopadhyay, Efficient Detection of Early Events of  $\alpha$ -Synuclein Aggregation Using a Cysteine Specific Hybrid Scaffold, *Biochemistry*. 58 (2019) 1109–1119. <https://doi.org/10.1021/acs.biochem.8b01161>.
- [50] A. Sarkar, A. Chakraborty, A. Adhikary, S. Maity, A. Mandal, D. Samanta, P. Ghosh, D. Das, Exploration of catecholase-like activity of a series of magnetically coupled transition metal complexes of Mn, Co and Ni: new insights into the solution state behavior of Mn complexes, *Dalt. Trans.* 48 (2019) 14164–14177. <https://doi.org/10.1039/C9DT02399B>.
- [51] E. Monzani, G. Battaini, A. Perotti, L. Casella, M. Gullotti, L. Santagostini, G. Nardin, L. Randaccio, S. Geremia, P. Zanello, G. Opromolla, Mechanistic, Structural, and Spectroscopic Studies on the Catecholase Activity of a Dinuclear Copper Complex by Dioxygen, *Inorg. Chem.* 38 (1999) 5359–5369. <https://doi.org/10.1021/ic990397b>.
- [52] K.D. Freeman-Cook, C. Autry, G. Borzillo, D. Gordon, E. Barbacci-Tobin, V. Bernardo, D. Briere, T. Clark, M. Corbett, J. Jakubczak, S. Kakar, E. Knauth, B. Lippa, M.J. Luzzio, M. Mansour, G. Martinelli, M. Marx, K. Nelson, J. Pandit, F. Rajamohan, S. Robinson, C. Subramanyam, L. Wei, M. Wythes, J. Morris, Design of Selective, ATP-Competitive Inhibitors of Akt, *J. Med. Chem.* 53 (2010) 4615–4622. <https://doi.org/10.1021/jm1003842>.
- [53] F. Perveen, N. Arshad, R. Qureshi, J. Nowsherwan, A. Sultan, B. Nosheen, H. Rafique, Electrochemical, spectroscopic and theoretical monitoring of anthracyclines' interactions with DNA and ascorbic acid by adopting two routes: Cancer cell line studies, *PLoS One*. 13 (2018) e0205764. <https://doi.org/10.1371/journal.pone.0205764>.
- [54] D.A. Köse, H. Necefoglu, Synthesis and characterization of bis(nicotinamide) m-hydroxybenzoate complexes of Co(II), Ni(II), Cu(II) and Zn(II), *J. Therm. Anal. Calorim.* 93 (2008) 509–514. <https://doi.org/10.1007/s10973-007-8712-5>.

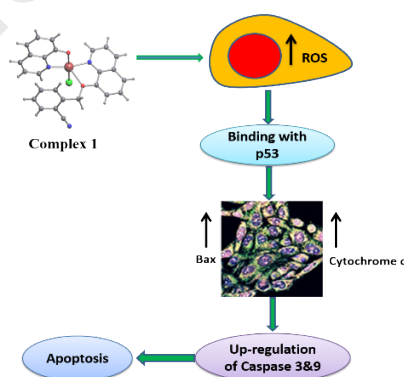
- [55] F. Sama, A.K. Dhara, M.N. Akhtar, Y.-C. Chen, M.-L. Tong, I.A. Ansari, M. Raizada, M. Ahmad, M. Shahid, Z.A. Siddiqi, Aminoalcohols and benzoates-friends or foes? Tuning nuclearity of Cu(II) complexes, studies of their structures, magnetism, and catecholase-like activities as well as performing DFT and TDDFT studies, *Dalt. Trans.* 46 (2017) 9801–9823. <https://doi.org/10.1039/C7DT01571B>.
- [56] A.W. Addison, T.N. Rao, J. Reedijk, J. van Rijn, G.C. Verschoor, Synthesis, structure, and spectroscopic properties of copper(II) compounds containing nitrogen–sulphur donor ligands; the crystal and molecular structure of aqua[1,7-bis(N-methylbenzimidazol-2'-yl)-2,6-dithiaheptane]copper(II) perchlorate, *J. Chem. Soc., Dalt. Trans.* (1984) 1349–1356. <https://doi.org/10.1039/DT9840001349>.
- [57] M.M. El-bendary, T. Ruffer, M.N. Arshad, A.M. Asiri, Synthesis and structure characterization of Pt(IV) and Cd(II) 1,10-phenanthroline complexes; fluorescence, antitumor and photocatalytic property, *J. Mol. Struct.* 1192 (2019) 230–240. <https://doi.org/10.1016/j.molstruc.2019.04.115>.
- [58] S.E.H. Etaiw, M.M. El-bendary, Hydrogen bonded 3D-network of silver and 2,6-pyridinedicarboxylic acid complex: Structure and applications, *J. Mol. Struct.* 1173 (2018) 7–16. <https://doi.org/10.1016/j.molstruc.2018.06.072>.
- [59] M.M. El-bendary, M.N. Arshad, A.M. Asiri, Structure characterization and antitumor activity of palladium pseudo halide complexes with 4-acetylpyridine, *J. Coord. Chem.* 72 (2019) 3088–3101. <https://doi.org/10.1080/00958972.2019.1683827>.
- [60] E. Brauchle, S. Thude, S.Y. Brucker, K. Schenke-Layland, Cell death stages in single apoptotic and necrotic cells monitored by Raman microspectroscopy, *Sci. Rep.* 4 (2015) 4698. <https://doi.org/10.1038/srep04698>.
- [61] F.L.S. H. -U. Simon, A. H. Yehia, Role of reactive oxygen species (ROS) in apoptosis induction, *Apoptosis.* 5 (2000) 415–418.
- [62] B. Brodská, A. Holoubek, Generation of Reactive Oxygen Species during Apoptosis Induced by DNA-Damaging Agents and/or Histone Deacetylase Inhibitors, *Oxid. Med. Cell. Longev.* 2011 (2011) 1–7. <https://doi.org/10.1155/2011/253529>.
- [63] S. Hekimi, Y. Wang, A. Noë, Mitochondrial ROS and the Effectors of the Intrinsic Apoptotic Pathway in Aging Cells: The Discerning Killers!, *Front. Genet.* 7 (2016) 161. <https://doi.org/10.3389/fgene.2016.00161>.

- [64] M. Morey, DIAP1 suppresses ROS-induced apoptosis caused by impairment of the selD/sps1 homolog in *Drosophila*, *J. Cell Sci.* 116 (2003) 4597–4604. <https://doi.org/10.1242/jcs.00783>.
- [65] J. Jiang, Z. Huang, Q. Zhao, W. Feng, N.A. Belikova, V.E. Kagan, Interplay between bax, reactive oxygen species production, and cardiolipin oxidation during apoptosis, *Biochem. Biophys. Res. Commun.* 368 (2008) 145–150. <https://doi.org/10.1016/j.bbrc.2008.01.055>.
- [66] C. Garrido, L. Galluzzi, M. Brunet, P.E. Puig, C. Didelot, G. Kroemer, Mechanisms of cytochrome c release from mitochondria, *Cell Death Differ.* 13 (2006) 1423–1433. <https://doi.org/10.1038/sj.cdd.4401950>.
- [67] H.M. Berens, K.L. Tyler, The Proapoptotic Bcl-2 Protein Bax Plays an Important Role in the Pathogenesis of Reovirus Encephalitis, *J. Virol.* 85 (2011) 3858–3871. <https://doi.org/10.1128/JVI.01958-10>.
- [68] S.E.H. Etaiw, M.M. El-bendary, Crystal structure, characterization and catalytic activities of Cu(II) coordination complexes with 8-hydroxyquinoline and pyrazine-2-carboxylic acid, *Appl. Organomet. Chem.* 32 (2018) e4213. <https://doi.org/10.1002/aoc.4213>.
- [69] A. Guha, T. Chattopadhyay, N.D. Paul, M. Mukherjee, S. Goswami, T.K. Mondal, E. Zangrando, D. Das, Radical Pathway in Catecholase Activity with Zinc-Based Model Complexes of Compartmental Ligands, *Inorg. Chem.* 51 (2012) 8750–8759. <https://doi.org/10.1021/ic300400v>.
- [70] K.S. Banu, T. Chattopadhyay, A. Banerjee, S. Bhattacharya, E. Suresh, M. Nethaji, E. Zangrando, D. Das, Catechol Oxidase Activity of a Series of New Dinuclear Copper(II) Complexes with 3,5-DTBC and TCC as Substrates: Syntheses, X-ray Crystal Structures, Spectroscopic Characterization of the Adducts and Kinetic Studies, *Inorg. Chem.* 47 (2008) 7083–7093. <https://doi.org/10.1021/ic701332w>.
- [71] I. Majumder, P. Chakraborty, S. Das, H. Kara, S.K. Chattopadhyay, E. Zangrando, D. Das, Solvent dependent ligand transformation in a dinuclear copper(II) complex of a compartmental Mannich-base ligand: synthesis, characterization, bio-relevant catalytic promiscuity and magnetic study, *RSC Adv.* 5 (2015) 51290–51301. <https://doi.org/10.1039/C5RA05776K>.
- [72] R. Sanyal, P. Kundu, E. Rychagova, G. Zhigulin, S. Ketkov, B. Ghosh, S.K. Chattopadhyay, E. Zangrando, D. Das, Catecholase activity of Mannich-based dinuclear

- Cu II complexes with theoretical modeling: new insight into the solvent role in the catalytic cycle, *New J. Chem.* 40 (2016) 6623–6635. <https://doi.org/10.1039/C6NJ00105J>.
- [73] M.N. Ahamad, M. Kumar, A. Ansari, M. I., M. Ahmad, M. Shahid, Synthesis, characterization, theoretical studies and catecholase like activities of  $[MO_6]$  type complexes, *New J. Chem.* 43 (2019) 14074–14083. <https://doi.org/10.1039/C9NJ03729B>.
- [74] A. Biswas, L.K. Das, M.G.B. Drew, G. Aromí, P. Gamez, A. Ghosh, Synthesis, Crystal Structures, Magnetic Properties and Catecholase Activity of Double Phenoxido-Bridged Penta-Coordinated Dinuclear Nickel(II) Complexes Derived from Reduced Schiff-Base Ligands: Mechanistic Inference of Catecholase Activity, *Inorg. Chem.* 51 (2012) 7993–8001. <https://doi.org/10.1021/ic202748m>.
- [75] M. Hassanein, S.E.H. Etaiw, S.H. El-Khalafy, M.M. El-bendary, Activity of Mixed Valence Copper Cyanide Metal–Organic Framework in the Oxidation of 3,5-di-Tert-Butylcatechol with Hydrogen Peroxide, *J. Inorg. Organomet. Polym. Mater.* 25 (2015) 664–670. <https://doi.org/10.1007/s10904-014-0139-4>.

### Graphical abstract

New copper(II) complex acts as a potential chemotherapeutic agent towards colorectal cancer.



**Research Highlights**

- New Cu(II)-based promising chemotherapeutic agent was synthesized and characterized.
- Complex **1** induces apoptosis in human colorectal carcinoma cell line (HCT116)
- Complex **1** serves as mimics of catechol oxidase
- Complex **1** could be acts as a promising scaffold for colon cancer

**Declaration of interests**

The authors declare that they have no known competing financial interests or personal relationships that could have appeared to influence the work reported in this paper.

The authors declare the following financial interests/personal relationships which may be considered as potential competing interests:



There are no conflicts of interest.

With regards

Dr. Mohd Afzal

Department of Chemistry

King Saud University, Riyadh

Email: maslam1@ksu.edu.sa